COVID-19 detection in chest X-ray images using deep boosted hybrid learning

Saddam Hussain Khan [a,b], Anabia Sohail [a,b], Asifullah Khan [a,b,c,*], Mehdi Hassan [d], Yeon Soo Lee [e,**], Jamshed Alam [f], Abdul Basit [g], Saima Zubair [h]

[a] Pattern Recognition Lab, Department of Computer & Information Sciences, Pakistan Institute of Engineering & Applied Sciences, Nilore, Islamabad, 45650, Pakistan
[b] PIEAS Artificial Intelligence Center (PAIC), Pakistan Institute of Engineering & Applied Sciences, Nilore, Islamabad, 45650, Pakistan
[c] Center for Mathematical Sciences, Pakistan Institute of Engineering & Applied Sciences, Nilore, Islamabad, 45650, Pakistan
[d] Department of Computer Science, Air University, Islamabad, Pakistan
[e] Department of Biomedical Engineering, College of Medical Science, Catholic University of Daegu, South Korea
[f] Medical Teaching Institute, Peshawar, Pakistan
[g] TPD, Pakistan Institute of Nuclear Science and Technology, Nilore, Islamabad, 45650, Pakistan
[h] Islamabad Institute of Reproduce Medicine, Pakistan

ARTICLE INFO

ABSTRACT

The new emerging COVID-19, declared a pandemic disease, has affected millions of human lives and caused a massive burden on healthcare centers. Therefore, a quick, accurate, and low-cost computer-based tool is required to timely detect and treat COVID-19 patients. In this work, two new deep learning frameworks: Deep Hybrid Learning (DHL) and Deep Boosted Hybrid Learning (DBHL), is proposed for effective COVID-19 detection in X-ray dataset. In the proposed DHL framework, the representation learning ability of the two developed COVID-RENet-1 & 2 models is exploited individually through a machine learning (ML) classifier. In COVID-RENet models, Region and Edge-based operations are carefully applied to learn region homogeneity and extract boundaries features. While in the case of the proposed DBHL framework, COVID-RENet-1 & 2 are fine-tuned using transfer learning on the chest X-rays. Furthermore, deep feature spaces are generated from the penultimate layers of the two models and then concatenated to get a single enriched boosted feature space. A conventional ML classifier exploits the enriched feature space to achieve better COVID-19 detection performance. The proposed COVID-19 detection frameworks are evaluated on radiologist's authenticated chest X-ray data, and their performance is compared with the well-established CNNs. It is observed through experiments that the proposed DBHL framework, which merges the two-deep CNN feature spaces, yields good performance (accuracy: 98.53%, sensitivity: 0.99, F-score: 0.98, and precision: 0.98). Furthermore, a web-based interface is developed, which takes only 5–10s to detect COVID-19 in each unseen chest X-ray image. This web-predictor is expected to help early diagnosis, save precious lives, and thus positively impact society.

1. Introduction

A pathogenic member of the coronavirus family, called severe acute respiratory syndrome coronavirus 2 (SAR-CoV-2), emerged in 2019, affected millions of people worldwide [1]. The disease caused by SAR-CoV-2 is known as COVID-19 and announced a pandemic by WHO [2]. The coronavirus family comprises a large number of viruses that causes mild respiratory illness to severe respiratory infections such as the Middle East respiratory syndrome [3].

COVID-19 is a highly infectious virus mainly affecting the respiratory system. The most common symptoms with COVID-19 are fever, cough and tiredness dyspnea. The disease may progress to involve the lower respiratory system, and here it causes severe inflammation in the lungs, causing pneumonia. Further progression to Acute respiratory distress

---

syndrome is not very uncommon in those affected with pneumonia leading to cytokines release syndrome, and consequently which lead to multi-organ failure and death [4,5]. COVID-19 spreads through respiratory droplets or aerosols secretion during cough, contact, etc., with the patient. Therefore, preventive measures, especially social distancing, wearing masks and quarantining the infected patient, have been suggested for the regulation of infection spread [6].

The detection of COVID-19 is determined through a laboratory approach that requires the suspected person to undergo a series of polymerase chain reaction (PCR) tests [7]. However, the former PCR based testing for COVID-19 screening is time-consuming and generates more false negatives [8,9]. Contrary to this, an advanced technological operation of radiographic imaging like X-rays is used as one of the quickest ways of detection [10]. COVID-19 infected patients are often screened through X-ray imaging to assess the infection spread in the lungs, patient management plan, and follow up [11].

The increased number of COVID-19 patients and its manual analysis of chest X-ray imaging have a significant burden on radiologists. Therefore, there is a need of developing an automatic system for the quick screening of COVID-19 infection and timely recovery [12]. Previously, several deep learning-based COVID-19 detection models have been designed and successfully deployed [13]. Among other machine learning (ML) techniques, well-established CNN models like GoogleNet, inception, Xception, etc., using transfer learning (TL), have been employed for detection [14,15].

Wang et al. developed the COVID-Net model to detect COVID-19 patients using X-ray images [16]. The COVID-Net achieved an accuracy (92%) and sensitivity (87%). Similarly, Afshar et al. presented the COVID-CAPS model and reported an accuracy of (98%) with a detection rate (80%) [17]. However, the models mentioned above achieved a low detection rate because of insufficient COVID-19 labelled datasets. Therefore, TL has been introduced in state-of-the-art models and fine-tuned on a problem-specific chest X-ray dataset. A state-of-the-art inception model using TL has been employed to screen COVID-19 with a low accuracy of (89.5%) [18]. Likewise, the pre-trained ResNet-50 CNN has been employed on a limited amount of samples and achieved an accuracy of (98%) [19]. Recently, an approach based on existing CNNs (ResNet18, squezeNet and DensNet201) has been used to detect COVID-19 patients. These models have been fine-tuned using TL on the "COVID-Xray-5k" dataset and reported 98% accuracy [20]. All the aforementioned models have been implemented on softmax-classifier for the screening of COVID-19 patients and thus, only exploited the benefits of empirical risk minimization.

Deep hybrid learning utilized both empirical and structural minimization benefits to improve the COVID-19 detection performance. In the related works [21,22], features are extracted from the existing ResNet-50 CNN model and provided fed to the ML classifier. This reported deep hybrid learning-based framework achieved an accuracy of (95%). Similarly, deep features from fine-tuned pre-trained ResNet-152 have been extracted and provided to ML classifiers. Similarly, COVID-19 detection using Random-Forest and XGBoost classifiers achieved an accuracy of (97.3%) and (97.7%), respectively [23].

Most of the previous works lack to tackle the following two main challenges:

1. Largely, existing CNN models have been employed on a limited chest X-ray dataset, which affects their performance on new and real-world datasets.
2. Additionally, these models have been designed specifically for natural images and fine-tuned for COVID-19 detection. COVID-19 infected images have a specific pattern and texture that differs from natural images. Usually, natural Images are large, simple in nature and distinctly different from each other [24]. Contrary to this, COVID-19 infection has a specific texture and pattern, and the extent of infection varies in patients. The patient with COVID-19 chest

infection shows patterns of ground-glass opacity, consolidation, and reticulation [13].

This study addressed the aforementioned research challenges by customizing the deep learning models to exploit COVID-19 specific texture and patterns using X-ray datasets. Deep learning models have shown exemplary performance on images compared to the shallow or conventional detection models. Therefore, the proposed COVID-19 detection scheme consists of two novel deep learning frameworks: Deep Hybrid Learning (DHL) and Deep Boosted Hybrid Learning (DBHL). In the proposed DHL framework, the deep feature learning capacity of the developed COVID-RENet-1 & 2 models is exploited individually through an SVM classifier to detect COVID-19 patients. While in the proposed DBHL framework consists of two developed base models, COVID-RENet-1 & 2, which is fine-tuned on the chest X-ray dataset using TL. Furthermore, the deep features are generated from the developed models and fused to get a single boosted feature space for training the SVM classifier to achieve enhanced performance. The COVID-RENets architectures are developed explicitly by looking into COVID-19 chest infection characteristics patterns. The key contributions of this work are as below:

1. The new DHL and DBHL frameworks are proposed for effective COVID-19 detection in chest X-ray images. In the proposed DHL framework, deep feature spaces are extracted from the penultimate layers of the developed COVID-RENet-1 & 2 model and individually given to the SVM classifier. In COVID-RENet models, Region and Edge-based operations are methodically employed to extract region homogeneity and boundaries features. Furthermore, TL has been utilized in the developed COVID-RENet models to enhance COVID-19 detection performance.
2. In the proposed DBHL framework, rich information boosted feature spaces are obtained by concatenating the deep feature spaces of both the developed TL-based COVID-RENet-1 & 2. Finally, the boosted deep features are reduced using PCA to get the most prominent feature set and is then provided to SVM, which has good pattern discrimination ability. In the proposed frameworks, the principle of structural and empirical risk minimization techniques are exploited to improve the discrimination power.
3. The performance of our proposed COVID-19 detection frameworks is compared with several well-established CNN models, and the proposed frameworks reduced significantly both false-negatives and false-positives.
4. A web predictor based on the proposed COVID-RENet model is developed to assist radiologists in making quick and accurate decisions.

The remaining of the paper proceeds as: In section 2, COVID-19 detection schemes are explained in detail. Section 3 discusses the experimental setup. The results are discussed in section 4, and section 5 concludes the study.

2. Proposed COVID-19 detection scheme

In this research, a novel deep learning COVID-19 detection scheme is proposed based on deep CNN and ML techniques. The proposed COVID-19 detection scheme employs three different experimental setups. During experimentation, training instances are augmented to increase the robustness of models. These augmented instances are utilized during the training of the proposed techniques. The workflow of COVID-19 detection schemes is illustrated in Fig. 1.

2.1. Dataset

In this work, a new chest X-ray dataset is constructed that contain healthy instances and COVID-19 patients. These dataset has been
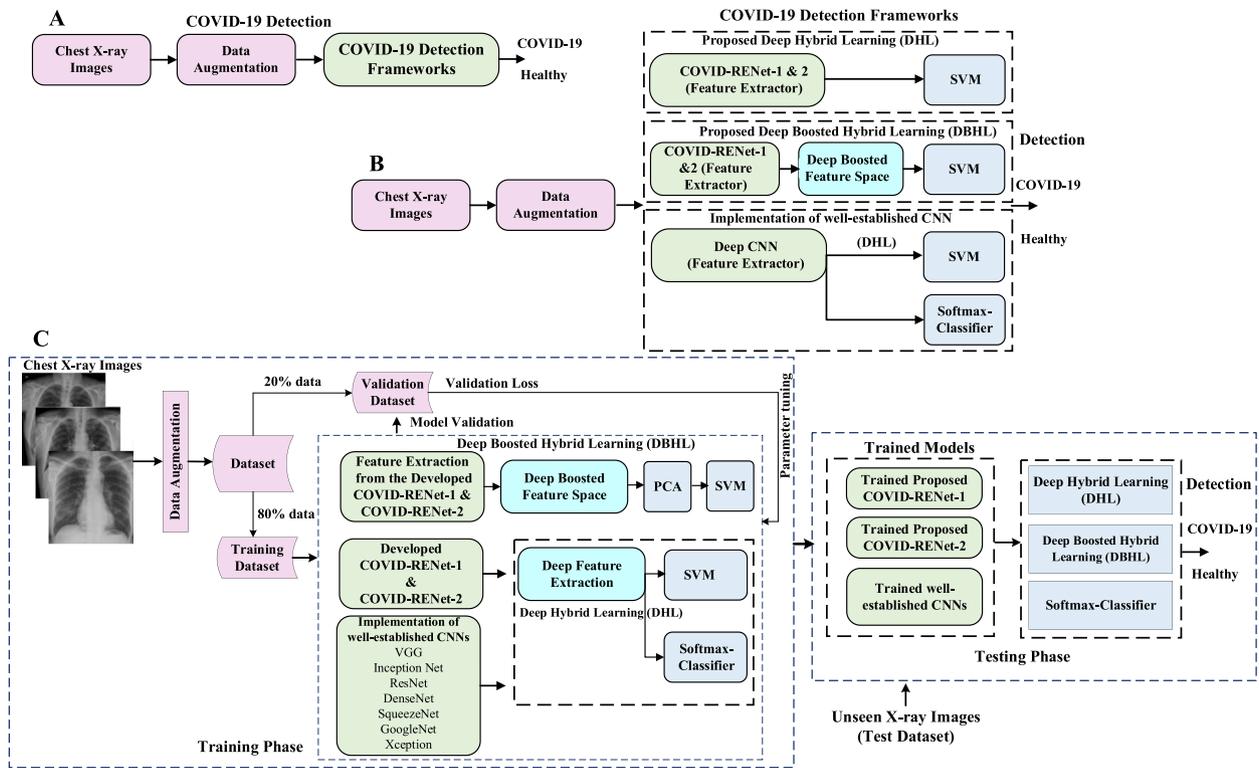
Fig. 1. Panels (A & B) shows the brief detail, while Panel (C) illustrate the detailed overview of the proposed COVID-19 detection schemes.

generated by collecting the publicly accessible X-ray images marked by radiologists in GitHub and Kaggle repositories [25,26]. The accessed repositories contain images from different regions, hospitals, and X-ray machines. The X-ray images have been captured at different positions and orientations relative to the X-ray source and detector panel. This work filters COVID-19 and healthy instances from the aforementioned repositories, as illustrated in Fig. 2. We have constructed a balanced dataset of 3224 COVID-19 infected and 3224 healthy instances. The images have different dimensions and are resized to 224 x 224 pixels.

2.2. Data augmentation

CNN architectures mostly overfit a smaller number of samples. Therefore, an enormous quantity of images is required for intensive training and improving the performance of models. Data augmentation strategy increases the data instances by performing different transformations on original data [27,28]. The implemented augmentation strategy includes rotation, reflection and scaling, as shown in Table 1.

Table 1
Data augmentation transformation and parameter values.

Augmentation	Parameters
Rotate	[0, 360] degrees
Reflection	X & Y: [- 1, 1]
Scale	[0.5, 1]

The employed augmented strategy on the X-ray training set improves the generalization and robustness of the COVID-19 detection framework.

2.3. COVID-19 detection framework

The proposed framework employs three different experimental setups for COVID-19 detection: (1) the proposed DHL, (2) The proposed DBHL, (3) the implementation of well-established CNN models. These
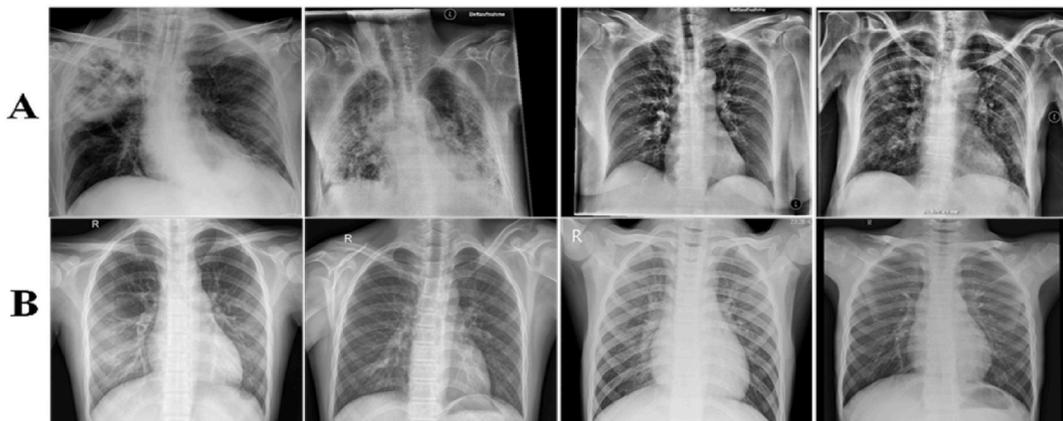

Fig. 2. Panel A illustrates the COVID-19 infected, while Panel B shows healthy instances.

well-established models are employed in two ways: (i) The deep features are generated from CNN models and assigned to SVM (DHL), (ii) The Softmax classifier-based implementation of the developed COVID-RENets and well-established CNNs for comparative studies. The aforementioned developed COVID-RENets and well-established CNNs are trained using TL as well as from scratch on the chest X-ray images.

2.3.1. Proposed deep hybrid learning (DHL) framework

In this work, two deep COVID-RENet-1 & 2 models are developed, and deep features space are extracted from the penultimate layers of these models and finally provided to SVM as shown in Figs. 3 and 4. In COVID-RENet models, Region and Edge-based operations are methodically employed to exploit region homogeneity and boundary related features. In this regard, we employ average and max-pooling operators, interleaving convolution operations in a systematic way for effective learning of the COVID-19 specific patterns [15].

The developed COVID-RENets are comprised of four feature extraction blocks. Each block contains convolutional layers and ReLU activation function as shown in Eq. (1) to exploit the spatial correlation by addressing non-linearity in the dataset. Every block is systematically followed by average (x^{avg}) and max pooling (x^{max}), to extract features corresponding to region homogeneity and edges, as illustrated in Eqs. (2 & 3). The systematic use of the region and edge-based implementations exhibit COVID-19 chest infection characteristics patterns.

$$x_{a,b} = \sum_{i=1}^{r} \sum_{j=1}^{s} x_{a+i-1,\ b+j-1} f_{i,j} \tag{1}$$

$$x^{avg}_{a,b} = \frac{1}{w^2} \sum_{i=1}^{w} \sum_{j=1}^{w} x_{a+i-1,\ b+j-1} \tag{2}$$

$$x^{max}_{a,b} = max_{i=1,...,w, j=1,...,w} x_{a+i-1,\ b+j-1} \tag{3}$$

$$x = \sum_{d}^{D} \sum_{c}^{C} u_d x_c \tag{4}$$

In Eq. (1), input channel and filter of dimension (A ×B) and r x s, are denoted by **x** and **f**, respectively. Where a and b ranges from 1 to A - r + 1 and B - s + 1, respectively. w denotes the window dimension of average and max-pooling, as illustrated in Eqs. (2 & 3). Whereas **u**$_d$ in Eq. (4) illustrates the number of neurons.

Deep hybrid learning utilized both empirical and structural minimization benefits to improve the COVID-19 detection performance. CNNs are well known for their strong learning abilities. These models focus on minimizing the training loss by reducing empirical risk factors that often lead to overfitting [29]. While, SVM is an ML classifier that minimizes structural risk factors, improving generalization by increasing the inter-class margin [30]. Therefore, the proposed DHL

framework consists of the deep features of CNN and SVM as a robust classifier. In this way, DHL exploits the learning potential of COVID-RENets that generates diverse features from X-ray images. Whereas, softmax in Eq. (5) is substituted with an SVM to improve the generalization.

2.3.2. Proposed deep boosted hybrid learning (DBHL) framework

Recently, in comparison, deep learning models have shown exemplary performance on images with shallow or conventional detection techniques [31]. Furthermore, feature boosting concatenates different individual models to get rich information features for better generalization performance. Therefore, the deep boosted hybrid learning-based model takes the benefit of both deep learning and ensemble learning. Finally, deep rich information feature space is provided to the generalized detection model [32].

In this regard, a DBHL framework has been proposed in which TL-based fine-tuned deep COVID-RENet- 1 & 2 CNNs are used as base models and SVM as a strong classifier. In the proposed DBHL framework, the deep feature spaces generated from both the developed COVID-RENets are ensembled to get enriched boosted feature spaces, as shown in Eq. (6). We generated 64 deep features from the second last flattened layer of the developed COVID-RENet-1 & 2 models and ensemble them into a 128-dimensional feature vector. After this, eigenvector based transformation is applied using principal component analysis (PCA) on deep boosted feature spaces (x_Boosted). PCA is a dimensionality reduction technique that tries to transform a large set of variables into uncorrelated smaller ones by preserving maximum information of the data set. PCA works by initially computing the covariance matrix from the dataset. Then, singular value decomposition of the covariance matrix has been performed to find the principal components. In PCA, eigenvector corresponds to the direction of maximum variance, while eigenvalue represent its magnitude. The principal components are ranked based upon their variance, and the top 32 components, which cover approximately 50% of the data variance have been selected. The PCA reduced feature space is provided to SVM for COVID-19 detection. The proposed framework DBHL for COVID-19 screening is illustrated in Fig. 5.

$$\sigma(\mathbf{x}) = \frac{e^{x_i}}{\sum_{i=1}^{K} e^{x_k}} \tag{5}$$

$$\mathbf{x}_{Boosted} = f_c(f_{RENet-1}(\mathbf{x}) || f_{RENet-2}(\mathbf{x})) \tag{6}$$

$$d(\lambda I - \mathbf{A}) = 0 \tag{7}$$

$$(\lambda \mathbf{I} - \mathbf{A})\mathbf{E} = 0 \tag{8}$$

In Eq. (5), σ and k denote the softmax activation function and the number of classes, respectively. Whereas **x** (Eq. (4)) is the extracted
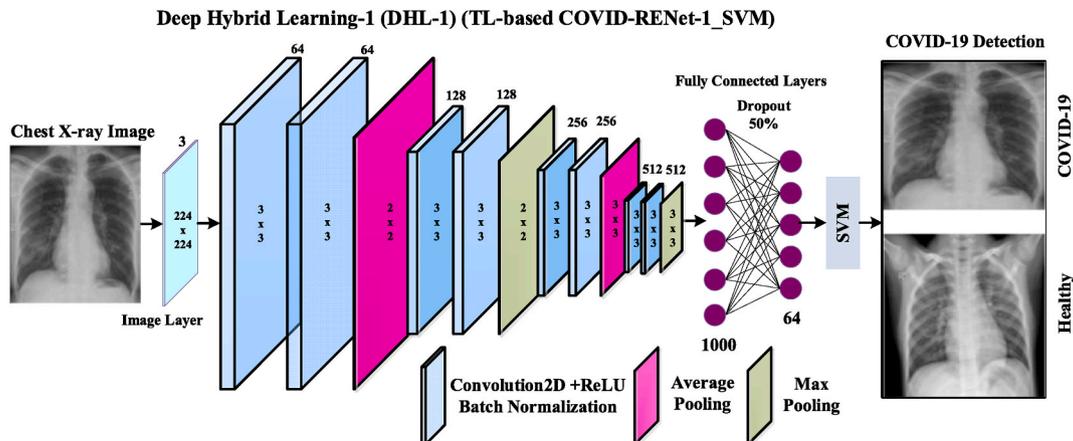

Deep Hybrid Learning-1 (DHL-1) (TL-based COVID-RENet-1_SVM)

Fig. 3. The proposed Deep Hybrid Learning-1 (DHL-1) framework for COVID-19 detection.

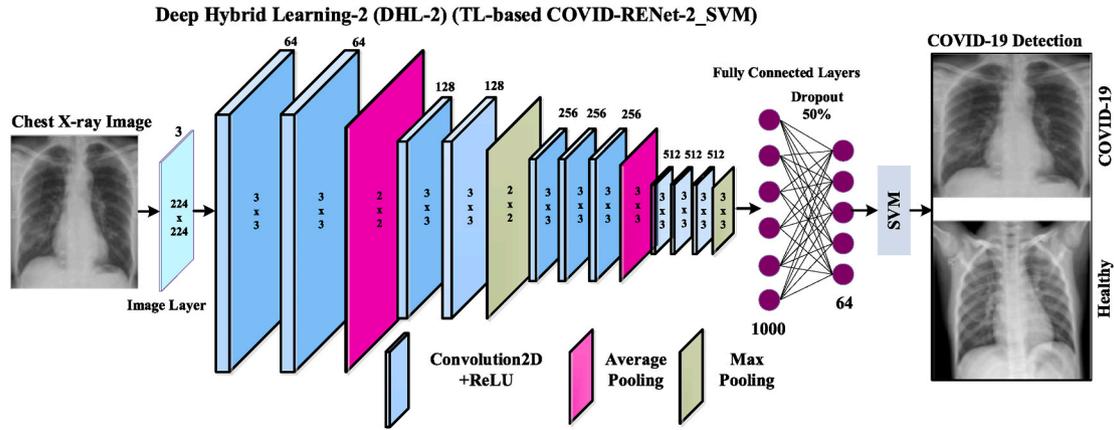**Deep Hybrid Learning-2 (DHL-2) (TL-based COVID-RENet-2_SVM)**

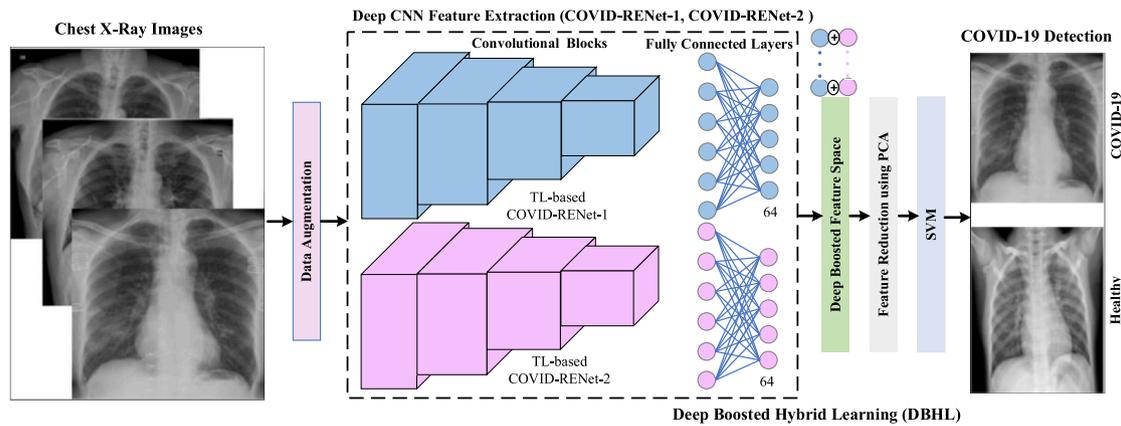**Fig. 4.** The proposed Deep Hybrid Learning-2 (DHL-2) framework for COVID-19 detection.

Fig. 5. The proposed Deep Boosted Hybrid Learning (DBHL) framework for COVID-19 detection.

features from the penultimate layer of COVID-RENets. The deep boosted feature space of COVID-RENet-1 & 2 is illustrated by Eq. (6). In PCA, the boosted feature space is normalized and then covariance matrix (**A**) is computed. Further, the eigenvalues and eigenvectors (principal components (PCs)) for the covariance matrix have been computed (Eqs. 7 & 8). I is the identity matrix of the same dimension as A and '*d*' is the determinant of the matrix. Finally, the top components that are expected to capture high variance, are selected and then provided to SVM.

$$\mathbf{w}^T\mathbf{x} + \mathbf{b} = 0 \tag{9}$$

$$\min_{w,\xi_i} C \sum_n^N \zeta_n + \frac{1}{2}\|\mathbf{w}\|^2 \tag{10}$$

In Eq. (9), the reduced feature space (**x**) is an input instance, whereas $\mathbf{w}^T$ and b is weight feature-space orthogonal to hyper-plane and bias, respectively. SVM constructs an optimal hyper-plane to minimize and maximize the intra and inter-class variation, respectively. As a resultant, it reduces the miss-classification rate, as shown in Eq. (10). ζ represents the miss-classified instances, while *C* is the misclassification cost that makes the trade-off between miss-classification and model generalization.

2.3.3. Implementation of the well-established CNNs

We implemented several existing CNN models for comparative analysis, including VGG-16/19, GoogleNet, InceptionV3, ResNet-18/50, SqueezeNet, DenseNet-201, and Xception [33–38]. Some of the CNNs have been previously employed for COVID-19 X-ray detection [39]. The comparison of complexity detail of the developed and well-established CNN models is shown in Table 2. These existing CNN models are

Table 2
Details of the proposed and well-established CNNs.

Model	Depth	Convolutional Layers	FC Layers
AlexNet	8	5	3
COVID-RENet-1	**11**	**8**	**3**
COVID-RENet-2	**13**	**10**	**3**
VGG-16	16	13	3
VGG-19	19	16	3
ResNet-18	22	20	2
SqueezeNet	28	26	2
ShuffleNet	51	49	2
ResNet-50	55	53	2
GoogleNet	59	57	2
Xception	75	74	2
Inception-V3	96	94	2
DesNet-201	203	201	2

customized by modifying the initial to be compatible with the input feature map dimensions.

A hybrid-based framework is incorporated in well-established CNN models to learn the deep feature hierarchies for ML-based detection. In this regard, an additional fully connected (FC) layer is added to fine-tune them for COVID-19 X-ray detection, and detection layers of these models are customized according to the target class category. Deep features are generated from the customized penultimate FC layer of existing CNNs and are assigned to SVM for detection. The feature dimension matrix of the feature extraction layer (second last customized FC layer) of the different well-established train from scratch and fine-tuned using TL CNN are 64x2. These models are also optimized in a Softmax-classifier-

based to extract the COVID-19 specific features from the chest dataset.

2.3.4. Training scheme of the detection models

The proposed COVID-RENets and well-established CNNs are primarily trained on chest X-ray data, randomly initializing parameters with uniform distribution. However, deep CNNs required an efficient amount of data. The insufficient amount of X-ray instances may cause lower convergence and affect COVID-19 detection performance [40]. Therefore, the concept of TL has been employed to achieve significant improvement in COVID-19 detection performance [41]. TL transfers the parameters of convolutional layers trained on the benchmark ImageNet dataset and adapted on the COVID-19 X-ray dataset. In this way, the parameters of the implemented models (COVID-RENets and well-established CNN) are initialized using TL. These models have been fine-tuned using domain-adaptation-based TL on the COVID-19 X-ray dataset [42,43]. We incorporated the hybrid framework where the convolutional layers of TL-based COVID-RENet-1 & 2 and well-established CNN extract COVID-19 image bottleneck features, which are then provided to the SVM classifier for training.

3. Experimental setup

3.1. Implementation details

The dataset is partitioned into separate datasets of training and testing at the ratio of 8:2 using hold-out cross-validation strategy. Furthermore, the training dataset has been split into training and validation sets at the same ratio (8:2). The validation set has been used for optimal hyper-parameters selection. After selecting the optimal hyper-parameters, CNN models have been trained with these parameters on the training set, and their values are mentioned in Table 3. In this work, we evaluated the performance of the proposed techniques on 4126, 1032, and 1290 number of training, validation and testing images, respectively.

All the CNN models have been designed and simulated on MATLAB-2021a. Dell model Core-i7-7500, 7th generation CPU, has been used for CNN model designing. Additionally, GPU-enabled Nvidia-GTX-1060-T has been utilized during training the CNN models. Each model training took almost 5–7 hrs, ~15–20 min/epoch.

3.2. Performance evaluation

The COVID-19 detection models have been evaluated using the standard performance metrics. The performance metric includes accuracy, sensitivity, specificity, and MCC. Accuracy calculates the correct detection of COVID-19 and Healthy instances, as demonstrated in Eq. (11). Sensitivity in eq. (12) measures the ratio of actual detected COVID-19 instances, while the specificity in Eq. (13) measures the actual predicted healthy instances. The precision and F-score is demonstrated in Eqs. (14) and (15), respectively. Finally, Mathews Correlation Coefficient (MCC) measures the quality of the confusion matrix and the F1-score measure the harmonic mean of precision and recall (sensitivity). The receiver operating characteristic (ROC) curve shows the performance of a detection model at different threshold values. ROC curve plot

Table 3
Selected hyper-parameters and its corresponding values.

Hyper-parameters	Values
Optimizer	SGDM
Momentum	0.95
Learning rate	0.0001
Weight decay	0.0005
Loss	Cross-entropy
Activation function	ReLU
Epoch	20
Batch size	16

sensitivity and 1- specificity rate. In Eq. (16) the standard error for ROC-AUC is computed at a 95% confidence interval (CI), where z = 1.96 [20,44].

$$\text{Accuracy} = \frac{\text{Detected COVID} - 19 + \text{Detected Healthy}}{\text{Total instances}} \times 100 \quad (11)$$

$$\text{Sensitivity} \Big/ \text{Recall(S)} = \frac{\text{Detected COVID} - 19}{\text{Total COVID} - 19 \text{ instances}} \times 100 \quad (12)$$

$$\text{Specificity} = \frac{\text{Detected Healthy}}{\text{Total Healthy instances}} \times 100 \quad (13)$$

$$\text{Precision(P)} = \frac{\text{Detected COVID} - 19}{\text{Detected COVID} - 19 + \text{Wrongly Detected COVID} - 19}$$
$$\times 100 \quad (14)$$

$$\text{F1} - \text{Score} = 2 \times \frac{\text{P} \times \text{S}}{\text{P} + \text{S}} \quad (15)$$

$$\text{CI} = z\sqrt{\frac{error(1 - error)}{Total\ instances}} \quad (16)$$

4. Results and discussion

In this work, two deep learning-based COVID-19 detection frameworks, namely DHL and DBHL, are proposed, and their performance is evaluated on the chest X-ray dataset.

4.1. Performance evaluation of the proposed framework

The results of our proposed DBHL and DHL frameworks are exhibited in Table 4 and Fig. 7. The proposed DHL-1 (TL-based COVID-RENet-1-SVM) framework correctly classified COVID-19 and healthy (COVID-19: 631, healthy: 635) instances. In comparison, the proposed DHL-2 (TL-based COVID-RENet-2-SVM) improved the sensitivity or true positives (COVID-19: 639, healthy: 628). The results suggest that TL improves the performance compared to training from scratch learning scheme for COVID-RENets, illustrated in Tables 4–5. Both the deep hybrid learning-based frameworks improve precision while maintaining sensitivity. Finally, the proposed DBHL framework efficiently discriminate both classes by enhancing the sensitivity while retaining precision (COVID-19: 641, healthy: 630).

4.2. Proposed frameworks comparison with well-established CNNs

The proposed frameworks performances, DBHL and DHL, are compared with well-established CNN models. Both the frameworks utilize the benefits of empirical and structural risk minimization techniques. The well-established CNN models are trained on the chest X-ray images using TL as well as from scratch. The comparison of standard performance metrics like accuracy, sensitivity, F-score, and MCC, is shown in detail in Figs. 6–7, Tables 4–7.

4.2.1. Proposed deep hybrid learning (DHL)

The performance comparison suggests that the proposed DHL framework better learn the COVID-19 infection pattern in X-ray images than well-established CNN models. The performance enhancement is due to the systematic usage of region and edge operation and SVM as the final detection model in the proposed framework. The developed COVID-RENet is based on the idea of region homogeneity and textural variation to effectively explore the COVID-19 patterns such as ground-glass opacity, consolidation, and reticulation. The systematic exploration of this information in X-Ray images helps differentiate the regular healthy region from the deformed region. Additionally, Region-based operations suppress noise for the deformations acquired during X-ray

Table 4

Performance of the proposed DBHL and DHL frameworks on the unseen dataset.

The proposed COVID-19 detection frameworks										
Model	AUC	F-score	MCC	Pre	Sen	Spec	Acc %	TP	FP	FN	TN
Deep Boosted hybrid Learning (DBHL)	0.99	0.98	0.97	0.98	0.99	0.98	98.53	641	15	**4**	630
Deep Hybrid Learning-2 (DHL-2)	0.99	0.98	0.97	0.97	0.99	0.97	98.29	639	17	**6**	628
Deep Hybrid Learning-1 (DHL-1)	0.99	0.98	0.96	0.98	0.98	0.98	98.14	631	10	**14**	635

Table 5

Performance of the developed COVID-19 detection models on the unseen dataset.

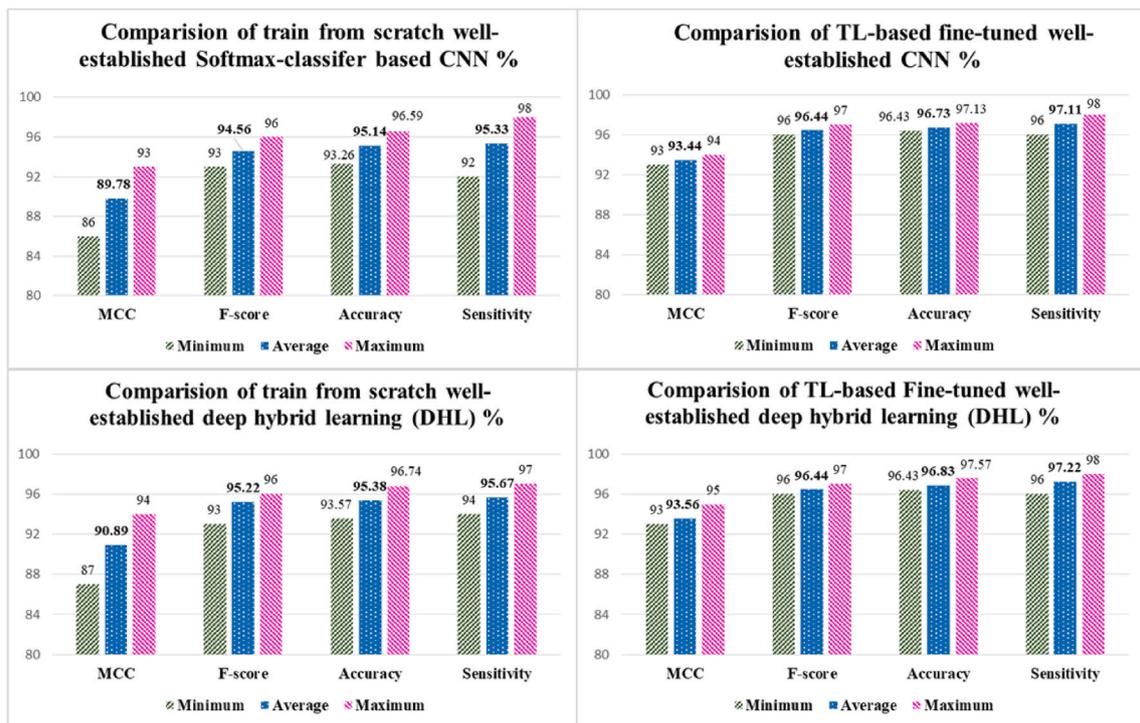| Softmax-classifier based the developed deep CNN models										
Model	AUC	F-score	MCC	Pre	Sen	Spec	Acc %	TP	FP	FN	TN
COVID-RENet-2	0.99	0.97	0.94	0.97	0.97	0.97	97.21	628	19	**17**	626
TL-COVID-RENet-2	0.99	0.98	0.96	0.98	0.98	0.98	98.14	633	12	**12**	633
COVID-RENet-1	0.99	0.97	0.94	0.97	0.97	0.97	97.21	627	18	**18**	627
TL COVID-RENet-1	0.99	0.98	0.96	0.99	0.97	0.99	98.06	628	8	**17**	637

Fig. 6. Performance comparison of hybrid based DHL and Softmax classifier-based implementation of well-established CNN models.
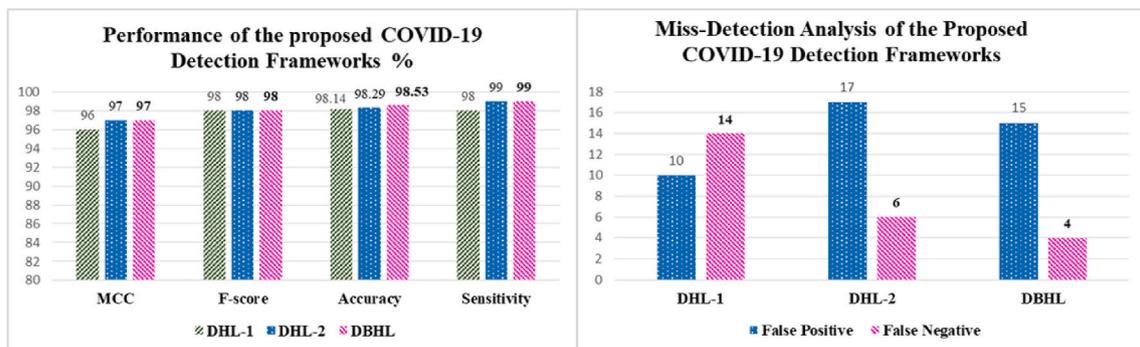

Fig. 7. Performance and miss-detection rate analysis of the proposed frameworks DBHL and DHL.

Table 6
Performance of well-established both trained from scratch and fine-tuned using TL CNNs on X-ray unseen dataset.

Models	AUC	F-score	MCC	Pre	Sen	Spec	Acc %	TP	FP	FN	TN
Squeeze Net	0.97	0.93	0.87	0.93	0.94	0.93	93.57	604	42	41	603
TL_Squeeze Net	0.98	0.96	0.93	0.96	0.97	0.96	96.59	626	25	19	620
VGG19	0.97	0.94	0.88	0.94	0.94	0.94	93.95	608	41	37	604
TL_VGG19	0.98	0.97	0.94	0.96	0.98	0.96	97.05	631	24	14	621
Inceptionv3	0.97	0.95	0.89	0.95	0.95	0.95	94.57	610	35	35	610
TL_Inceptionv3	0.98	0.96	0.93	0.97	0.96	0.97	96.43	619	20	26	625
Google Net	0.98	0.95	0.91	0.95	0.96	0.95	95.51	619	32	26	613
TL_Google Net	0.98	0.96	0.93	0.96	0.97	0.96	96.59	625	24	20	621
VGG16	0.98	0.96	0.92	0.96	0.96	0.96	95.81	619	28	26	617
TL_ VGG16	0.98	0.97	0.94	0.97	0.98	0.97	97.13	629	21	16	624
DenseNet201	0.98	0.96	0.92	0.96	0.96	0.96	95.97	618	25	27	620
TL_DenseNet201	0.98	0.96	0.93	0.96	0.97	0.96	96.43	625	26	20	619
Xception	0.98	0.96	0.92	0.96	0.96	0.96	95.97	622	29	23	616
TL_Xception	0.99	0.96	0.93	0.96	0.97	0.96	96.67	627	25	18	620
Resnet50	0.98	0.96	0.93	0.96	0.97	0.96	96.36	627	29	18	616
TL_Resnet50	0.99	0.97	0.94	0.97	0.97	0.97	97.05	628	21	17	624
Resnet18	0.99	0.96	0.94	0.96	0.97	0.96	96.74	626	23	19	622
TL_Resnet18	0.99	0.97	0.95	0.97	0.98	0.97	97.57	631	18	14	627

Table 7
Performance of well-established both trained from scratch and fine-tuned using TL CNNs on X-ray unseen dataset.

Models	AUC	F-score	MCC	Pre	Sen	Spec	Accuracy %	TP	FP	FN	TN
Squeeze Net	0.97	0.93	0.86	0.92	0.95	0.92	93.26	612	54	33	591
TL_Squeeze Net	0.98	0.96	0.93	0.96	0.97	0.96	96.51	625	25	20	620
VGG19	0.97	0.93	0.87	0.92	0.95	0.92	93.64	614	51	31	594
TL_VGG19	0.98	0.97	0.94	0.96	0.98	0.96	96.90	629	24	16	621
Inceptionv3	0.97	0.93	0.86	0.95	0.92	0.95	93.80	595	30	50	615
TL_Inceptionv3	0.98	0.96	0.93	0.97	0.96	0.97	96.51	620	20	25	625
Google Net	0.98	0.95	0.91	0.95	0.96	0.95	95.50	618	31	27	614
TL_Google Net	0.98	0.96	0.93	0.96	0.97	0.96	96.51	626	26	19	619
VGG16	0.98	0.95	0.91	0.96	0.95	0.96	95.74	615	25	30	620
TL_ VGG16	0.98	0.96	0.93	0.97	0.96	0.97	96.51	621	21	24	624
DenseNet201	0.98	0.95	0.91	0.94	0.97	0.94	95.74	627	37	18	608
TL_DenseNet201	0.98	0.96	0.93	0.96	0.97	0.96	96.43	625	26	20	619
Xception	0.98	0.95	0.91	0.96	0.95	0.96	95.74	615	25	30	620
TL_Xception	0.98	0.97	0.94	0.97	0.97	0.97	97.05	628	21	17	624
Resnet50	0.98	0.96	0.92	0.95	0.98	0.95	96.28	631	34	14	611
TL_Resnet50	0.99	0.97	0.94	0.97	0.98	0.97	97.05	629	22	16	623
Resnet18	0.98	0.96	0.93	0.98	0.95	0.98	96.59	611	10	34	635
TL_Resnet18	0.99	0.97	0.94	0.97	0.98	0.97	97.13	629	21	16	624

imaging [10]. Moreover, SVM reduces structural risk minimization, which improves generalization by increasing the margin between inter-classes.

4.2.2. Proposed deep boosted hybrid learning (DBHL)
The performance of the proposed DBHL framework is compared with the proposed DHL. The proposed DBHL framework achieved the highest detection performance (98.53%, MCC: 0.97, sensitivity: 0.99, and precision 0.98) as shown in Table 4 and Fig. 7. In the DBHL framework, we extract deep features from the two developed base models (COVID-RENet-1 & 2) and boost the deep features by feature fusing. Further, the prominent feature set is achieved by employing PCA on the deep boosted features and then provided to SVM. The DBHL framework produces better precision, recall, F-Score, and accuracy than any deep CNN model. The proposed DBHL framework attained improvement almost, MCC (3–11%), sensitivity (1–7%), accuracy (1–5.27%), and F1-Score (1–5%) in overall the implemented well-established CNN models (detail result shown in Tables 4–7 and Figs. 6–7). This newly proposed DBHL framework is expected to make the COVID-19 detection more robust and highly efficient for the COVID-19 chest-related infections.

4.3. Performance evaluation of the well-established CNNs
To effectively evaluate the potential of existing CNNs, these models have been trained both from scratch and fine-tuned using TL on the chest X-ray images. TL allows reusing weight space of the already trained models to prevent the deep CNNs from under-fitting and stucking in local minima by providing good initial weights. Furthermore, TL prevents highly parameterized models from over-fitting by delivering knowledge from the different source domains and achieve good generalization in the target domain [45]. Therefore, TL is employed to effectively train the well-established CNNs to learn the COVID-19 specific features. It is noticed that the TL-based fine-tuned perform better than the trained from scratch CNN models with additional customized layers (results shown in Table 4).

Lastly, the integration of CNN's powerful deep feature learning capacity with the good generalization ability of the SVM is employed. In this way, we detected the COVID-19 X-ray images by generating the deep feature space from the well-established CNN models like VGG-16/19, InceptionV3, ResNet-18/50, DenseNet-201 and SqueezeNet. These deep features are then provided to SVM, which have a strong pattern

discrimination ability. To identify the significance of exploitation of deep feature engineering, for comparison purposes, we have used a Softmax classifier-based implementation of existing CNN models as well. The DHL technique performs better than the Softmax classifier-based implementation, as shown in Tables 6–7 Whereas, among the existing CNN models, TL based fine-tuned models perform better than models trained from scratch in both the strategies, including DHL and Softmax classifier-based detection (Fig. 6, Tables 6–7). Fig. 6 illustrates the minimum, average, and maximum performance of each metric.

4.4. Detection rate analysis

The effectiveness of COVID-19 detection models is usually evaluated through sensitivity and precision metrics. These metrics are important in controlling the spread of COVID-19 infection. Therefore, in the proposed frameworks, sensitivity and precision are computed for unseen chest X-ray images, as depicted in Tables 4–5

The empirical evaluation illustrates that the proposed hybrid based DHL framework outperforms the well-established techniques. In this connection, we further improve the detection rate by boosting the deep feature space of the developed COVID-RENet-1 & 2 models. The proposed DBHL framework correctly identified COVID-19 patients within a negligible time and reduced the miss-predictions, as shown in Fig. 7 and Table 4. Comparing the proposed DBHL framework with the proposed DHL and existing CNN techniques, the proposed framework achieved

the highest detection rate (0.99, False-negative = 4) with fewer False-positive. Additionally, it also significantly improves the detection system's precision (0.98) and, as a result, less burden on the radiologist.

The X-ray samples which are miss-detected by the proposed frameworks are may be due to complex patterns, contrast variation, and intricate instances, as shown in Fig. 7. However, several preprocessing methods like data augmentation are employed during training to maximize the detection performance. For this reason, we augmented the chest X-ray images by using different image transformation schemes in order to improve the model generalization.

4.5. Feature set visualization

Deep features learnt by the proposed frameworks DHL and DBHL are investigated to interpret classification process. Generally, the model discrimination ability is related to the traits of the feature set. Class discriminant features increase the model's learning capacity and robustness on a diverse set of instances. The proposed DBHL significantly enhanced the feature diversity and, consequently, improved the COVID-19 detection. The 2D scatter plots of the PCs and their percentage variance of the proposed frameworks DHL and DBHL on unseen data are shown in Fig. 8. PCA-based feature visualization of the unseen set suggests that the proposed frameworks have shown a good distinction between COVID-19 and healthy instances.
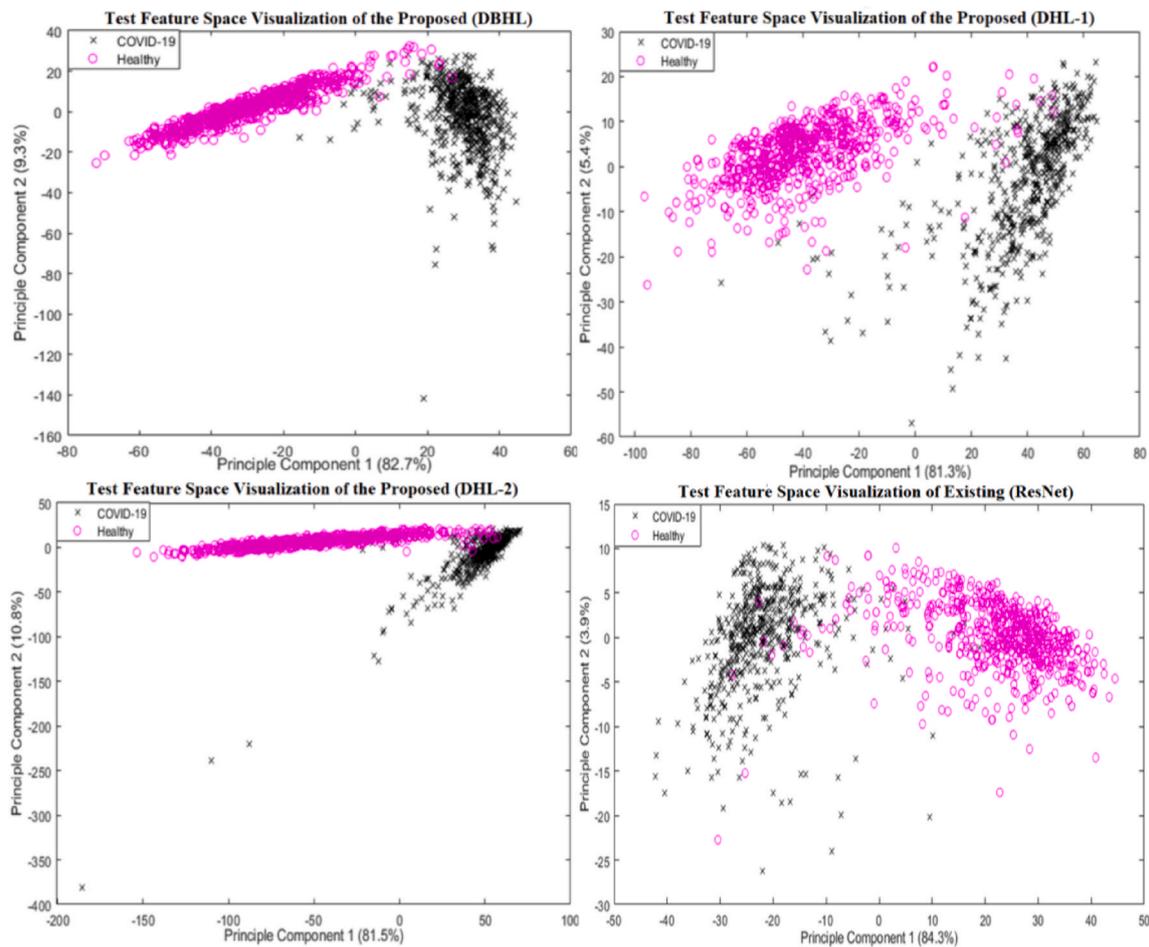

Fig. 8. Feature Visualization of the proposed COVID-19 detection frameworks DHL, DBHL, and the best performing well-established ResNet.

4.6. ROC based analysis

ROC curve plays a significant role in analysing classifiers strength for separating COVID-19 infected and healthy instances. The discrimination ability of the proposed approaches at different threshold values was analysed using ROC; thus, a radiologist may select the optimal value of interest [46]. Fig. 9 shows that the proposed frameworks DHL and DBHL achieved high AUC (0.99) on the X-ray dataset. This quantitative analysis manifests that the DBHL framework achieved the highest sensitivity and specificity. The graphical and quantitative analysis suggests that the proposed frameworks have a significant potential to deploy for COVID-19 detection.

4.7. COVID-19 web predictor

A web predictor tool based on the developed COVID-RENet model is designed to analyze COVID-19 in chest X-ray images. The web-predictor allows the radiologist to upload a chest X-ray image to the predictor. The proposed model will execute on chest X-ray at the backhand and gives the model prediction. As a result, the prediction can be COVID-19 positive (1) or negative (0) along with their confidence score, as illustrated in Fig. 10. The web predictor may be utilized in any COVID healthcare center for quick and accurate COVID-19 detection. The web predictor for COVID-19 detection, along with its implementation details, is publicly available at https://covid-xray-clf.herokuapp.com/.

5. Conclusions

Fast and early detection of COVID-19 patients is necessary to avoid spreading the disease. In this study, a novel DHL and DBHL framework is proposed to detect COVID-19 in chest X-ray images effectively. The proposed DBHL benefits from data augmentation, TL-based fine-tuning, deep features boosting, and hybrid learning from the developed COVID-RENets. In this regard, two deep CNN models (COVID-RENets-1 & 2) have been adopted for feature boosting and hybrid learning to detect COVID-19 accurately. Deep feature boosting help in merging the potentials of developed COVID-RENets models while overcoming the deficits of the individual COVID-RENet model. Experimental results demonstrated that the proposed DBHL framework performs better than competitive well-established CNN models in terms of accuracy, F-score, MCC, and recall. DBHL achieved an accuracy of 98.53% for the segregation of COVID-19 infected and healthy instances with 0.99 sensitivity and 0.98 specificity, respectively. The proposed DBHL framework and the web-predictor interface can efficiently assist the radiologists as it takes only 5–10s to predict COVID-19 infection in chest X-ray image. Quick and computer-aided diagnosis using the proposed framework may help in saving valuable lives and thereby have a positive socio-economic impact on society. In the future, an effort will be made to evaluate the DBHL framework on the multi-class dataset and deploy the computer-based tool in healthcare centers.
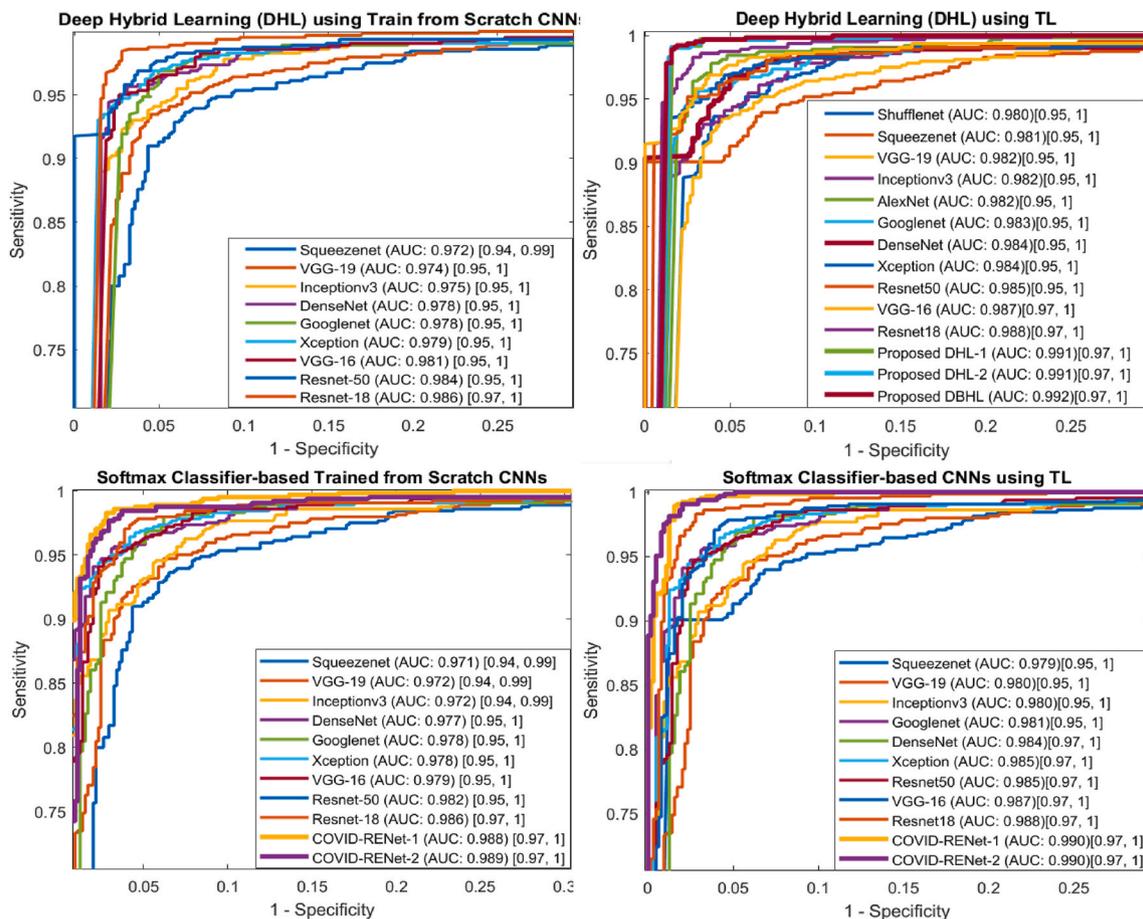

Fig. 9. ROC curve for the proposed frameworks (DHL, DBHL), the developed and well-established CNN Models. The square bracket values represent the tolerance or error, calculated at a 95% confidence interval [44].
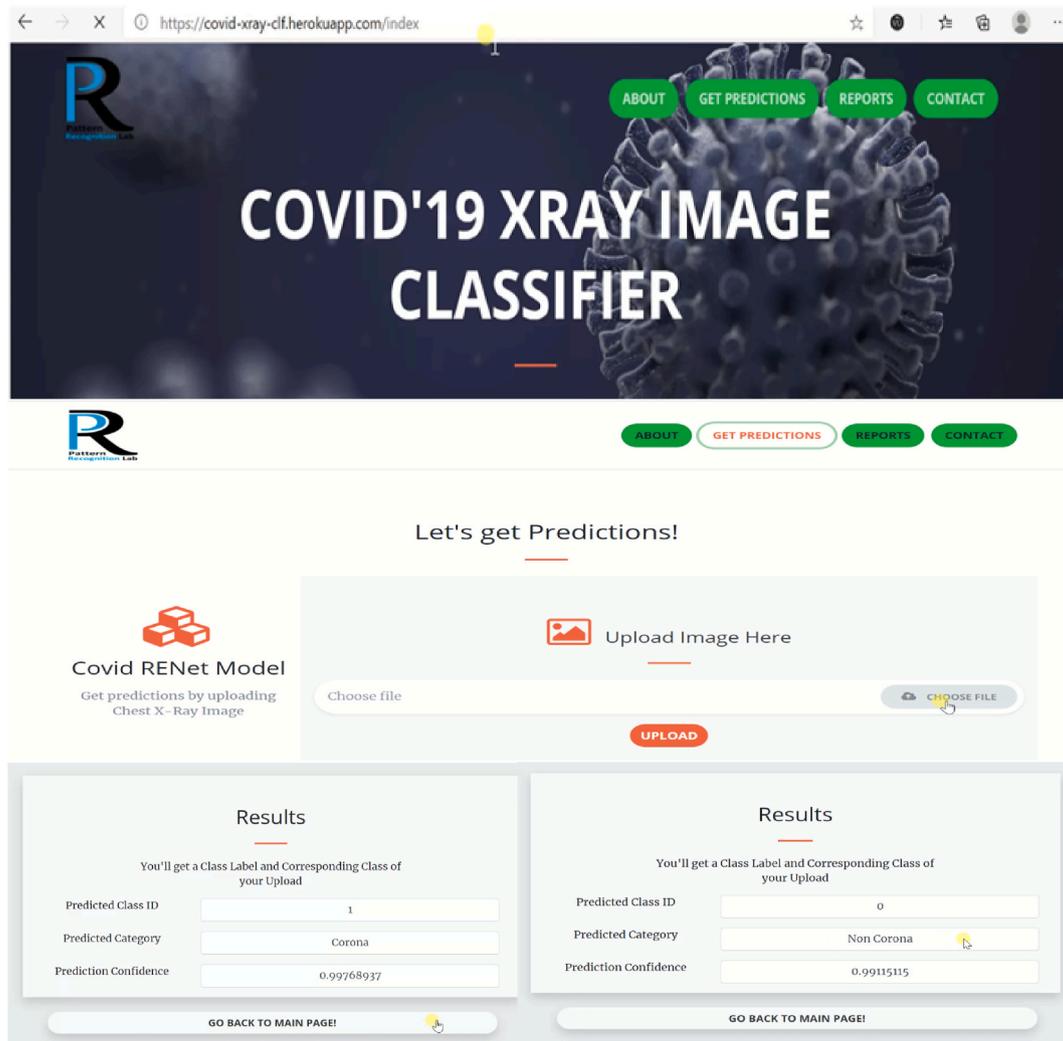
Fig. 10. COVID-19 web predictor, where 1 and 0 represents COVID-19 and Non-COVID instances on unseen stringent dataset, respectively.

Availability of data and material

Publicly available dataset is used in this work that is accessible at https://www.kaggle.com/khoongweihao/covid19-xray-dataset-train-test-sets and https://github.com/ieee8023/covid-chestxray-dataset. Whereas all the data generated during analysis is accessible from corresponding author on reseasonable request.

Code availability

All the scripts that are developed for the simulations are available from the corresponding author on reasonable request.

Declaration of interests

The authors declare that they have no known competing financial interests or personal relationships that could have appeared to influence the work reported in this paper.

Declaration of competing interest

Authors declare no conflict of interest.

References

[1] L. Pang, S. Liu, X. Zhang, T. Tian, Z. Zhao, TRANSMISSION DYNAMICS and CONTROL STRATEGIES of COVID-19 in WUHAN, China, J. Biol. Syst. 28 (3) (2020) 543–560, https://doi.org/10.1142/S0218339020500096.

[2] J. Zheng, SARS-coV-2: an emerging coronavirus that causes a global threat, Int. J. Biol. Sci. 16 (10) (2020) 1678–1685, https://doi.org/10.7150/ijbs.45053.

[3] M.A. Shereen, S. Khan, A. Kazmi, N. Bashir, R. Siddique, COVID-19 infection: origin, transmission, and characteristics of human coronaviruses, J. Adv. Res. 24 (2020) 91–98, https://doi.org/10.1016/j.jare.2020.03.005.

[4] A. Venyo, COVID-19 pneumonia: a review of typical ct findings and differential diagnosis, Biomedical Research and Clinical Reviews 1 (3) (2020), https://doi.org/10.31579/2692-9406/019, 01–22.

[5] S. Zaim, J.H. Chong, V. Sankaranarayanan, A. Harky, COVID-19 and multiorgan response, Curr. Probl. Cardiol. (2020), https://doi.org/10.1016/j.cpcardiol.2020.100618. http://www.embase.com/search/results?subaction=viewrecord&from=export&id=L2005924566%0A.

[6] J.A. Lewnard, N.C. Lo, Scientific and ethical basis for social-distancing interventions against COVID-19, Lancet Infect. Dis. 20 (6) (2020) 631–633, https://doi.org/10.1016/S1473-3099(20)30190-0.

[7] Y. Wang, H. Kang, X. Liu, Z. Tong, Combination of RT-qPCR testing and clinical features for diagnosis of COVID-19 facilitates management of SARS-CoV-2 outbreak, J. Med. Virol. 92 (6) (2020) 538–539, https://doi.org/10.1002/jmv.25721.

[8] A. Afzal, Molecular diagnostic technologies for COVID-19: limitations and challenges, J. Adv. Res. 26 (2020) 149–159, https://doi.org/10.1016/j.jare.2020.08.002.

[9] L. Hao-Chih, et al., Artificial intelligence–enabled rapid diagnosis of patients with COVID-19, Nat. Med. 26 (8) (2020) 1224–1228. http://search.proquest.com/docview/2432263836/.

[10] S.H. Khan, A. Sohail, A. Khan, Y.S. Lee, Classification and Region Analysis of COVID-19 Infection Using Lung CT Images and Deep Convolutional Neural Networks, Sep. 2020. http://arxiv.org/abs/2009.08864.

[11] M.E.H. Chowdhury, et al., Can AI help in screening viral and COVID-19 pneumonia? IEEE Access 8 (Mar. 2020) 132665–132676, https://doi.org/10.1109/ACCESS.2020.3010287.

[12] T. Mahmud, M.A. Rahman, S.A. Fattah, CovXNet: a multi-dilation convolutional neural network for automatic COVID-19 and other pneumonia detection from chest X-ray images with transferable multi-receptive feature optimization, Comput. Biol. Med. 122 (2020), https://doi.org/10.1016/j.compbiomed.2020.103869.

[13] Z. Wang, et al., Automatically discriminating and localizing COVID-19 from community-acquired pneumonia on chest X-rays, Pattern Recogn. 110 (2021), https://doi.org/10.1016/j.patcog.2020.107613.

[14] T. Ozturk, M. Talo, E.A. Yildirim, U.B. Baloglu, O. Yildirim, U. Rajendra Acharya, Automated detection of COVID-19 cases using deep neural networks with X-ray images, Comput. Biol. Med. 121 (2020), https://doi.org/10.1016/j.compbiomed.2020.103792.

[15] S.H. Khan, A. Sohail, M.M. Zafar, A. Khan, Coronavirus disease analysis using chest X-ray images and a novel deep convolutional neural network, Photodiagnosis Photodyn. Ther. 35 (April) (Sep. 2021) 102473, https://doi.org/10.1016/j.pdpdt.2021.102473.

[16] L. Wang, Z.Q. Lin, A. Wong, COVID-Net: a tailored deep convolutional neural network design for detection of COVID-19 cases from chest X-ray images, Sci. Rep. 10 (2020), https://doi.org/10.1038/s41598-020-76550-z.

[17] P. Afshar, S. Heidarian, F. Naderkhani, A. Oikonomou, K.N. Plataniotis, A. Mohammadi, COVID-CAPS: a capsule network-based framework for identification of COVID-19 cases from X-ray images, 2020, pp. 1–5.

[18] S. Wang, et al., A Deep Learning Algorithm Using CT Images to Screen for Corona Virus Disease (COVID-19), Apr. 2020, https://doi.org/10.1101/2020.02.14.20023028 medRxiv, p. 2020.02.14.20023028.

[19] Ali Narin, C. Kaya, Ziynet Pamuk, Automatic detection of coronavirus disease (COVID-19) using X-ray images and deep convolutional neural networks, Computer Vision and Pattern Recognition (2020).

[20] S. Minaee, R. Kafieh, M. Sonka, S. Yazdani, G. Jamalipour Soufi, Deep-COVID: predicting COVID-19 from chest X-ray images using deep transfer learning, Med. Image Anal. 65 (2020), https://doi.org/10.1016/j.media.2020.101794.

[21] P.K. Sethy, S.K. Behera, P.K. Ratha, P. Biswas, Detection of coronavirus disease (COVID-19) based on deep features and support vector machine, International Journal of Mathematical, Engineering and Management Sciences 5 (4) (2020) 643–651, https://doi.org/10.33889/IJMEMS.2020.5.4.052.

[22] S.H. Khan, M.H. Yousaf, F. Murtaza, S. Velastin, Passenger detection and counting for public transport system, NED Univ. J. Res. XVII (2) (2020) 35–46, https://doi.org/10.35453/nedjr-ascn-2019-0016.

[23] R. Kumar, R. Arora, V. Bansal, V.J. Sahayasheela, Accurate prediction of COVID-19 using chest X-ray images through deep feature learning model with SMOTE and machine learning classifiers, 2020, pp. 1–10, https://doi.org/10.1101/2020.04.13.20063461.

[24] N. Ahmad, S. Hussain, K. Ahmad, N. Conci, Computer Vision Based Room Interior Design, Dec. 2015, p. 98751G, https://doi.org/10.1117/12.2228438.

[25] COVID-19 Xray Dataset (Train & Test Sets) | Kaggle." .

[26] J.P. Cohen, P. Morrison, L. Dao, COVID-19 Image Data Collection, Mar. 2020.

[27] C. Shorten, T.M. Khoshgoftaar, A survey on image data augmentation for deep learning, Journal of Big Data 6 (1) (2019), https://doi.org/10.1186/s40537-019-0197-0.

[28] L. Perez, J. Wang, The Effectiveness of Data Augmentation in Image Classification Using Deep Learning, 2017. http://arxiv.org/abs/1712.04621.

[29] N. Wahab, A. Khan, Multifaceted fused-CNN based scoring of breast cancer whole-slide histopathology images, Applied Soft Computing Journal 97 (2020), https://doi.org/10.1016/j.asoc.2020.106808.

[30] H. Faris, M.A. Hassonah, A.M. Al-Zoubi, S. Mirjalili, I. Aljarah, A multi-verse optimizer approach for feature selection and optimizing SVM parameters based on a robust system architecture, Neural Comput. Appl. 30 (8) (2018) 2355–2369, https://doi.org/10.1007/s00521-016-2818-2.

[31] A. Khan, A. Sohail, U. Zahoora, A.S. Qureshi, A survey of the recent architectures of deep convolutional neural networks, Artif. Intell. Rev. (Apr. 2020) 1–68, https://doi.org/10.1007/s10462-020-09825-6.

[32] A. Sohail, A. Khan, H. Nisar, S. Tabassum, A. Zameer, Mitotic nuclei analysis in breast cancer histopathology images using deep ensemble classifier, Med. Image Anal. 72 (Aug. 2021) 102121, https://doi.org/10.1016/j.media.2021.102121.

[33] A. Khan, A. Sohail, U. Zahoora, A.S. Qureshi, A Survey of the Recent Architectures of Deep Convolutional Neural Networks, 2019 arXiv.

[34] K. Simonyan, A. Zisserman, Very deep convolutional networks for large-scale image recognition, in: 3rd International Conference on Learning Representations, ICLR 2015 - Conference Track Proceedings, 2015, pp. 1–14.

[35] F.N. Iandola, M.W. Moskewicz, K. Ashraf, S. Han, W.J. Dally, K. Keutzer, SqueezeNet, 2016 arXiv.

[36] R.W. Fairclough, et al., Going deeper with convolutions, IEEE Comput. Soc. Conf. Comput. Vis. Pattern Recogn. 40 (1) (2015) 1–9.

[37] C. Szegedy, V. Vanhoucke, S. Ioffe, J. Shlens, Z. Wojna, Rethinking the inception architecture for computer vision, IEEE Comput. Soc. Conf. Comput. Vis. Pattern Recogn. (2016) 2818–2826, https://doi.org/10.1109/CVPR.2016.308, 2016-Decem.

[38] N. Chouhan, A. Khan, J.Z. Shah, M. Hussnain, M.W. Khan, Deep convolutional neural network and emotional learning based breast cancer detection using digital mammography, Comput. Biol. Med. 132 (2021), https://doi.org/10.1016/j.compbiomed.2021.104318.

[39] A.A. Ardakani, A.R. Kanafi, U.R. Acharya, N. Khadem, A. Mohammadi, Application of deep learning technique to manage COVID-19 in routine clinical practice using CT images: results of 10 convolutional neural networks, Comput. Biol. Med. 121 (2020), https://doi.org/10.1016/j.compbiomed.2020.103795.

[40] H. Chougrad, H. Zouaki, O. Alheyane, Multi-label transfer learning for the early diagnosis of breast cancer, Neurocomputing 392 (2020) 168–180, https://doi.org/10.1016/j.neucom.2019.01.112.

[41] U. Ahmed, A. Khan, S.H. Khan, A. Basit, I.U. Haq, Y.S. Lee, Transfer Learning and Meta Classification Based Deep Churn Prediction System for Telecom Industry, 2019 arXiv.

[42] A. Sohail, A. Khan, N. Wahab, A. Zameer, S. Khan, A multi-phase deep CNN based mitosis detection framework for breast cancer histopathological images, Sci. Rep. 11 (2021), https://doi.org/10.1038/s41598-021-85652-1.

[43] A. Khan, A.S. Qureshi, N. Wahab, M. Hussain, M.Y. Hamza, A Recent Survey on the Applications of Genetic Programming in Image Processing, 2019, https://doi.org/10.1111/coin.12459.

[44] Confidence Intervals for Machine Learning." https://machinelearningmastery.com/confidence-intervals-for-machine-learning/(accessed Jun. 23, 2021).

[45] S.H. Khan, A. Sohail, A. Khan, COVID-19 Detection in Chest X-Ray Images Using a New Channel Boosted CNN, arXiv, 2020, http://arxiv.org/abs/2012.05073.

[46] Karimollah Hajian Tilaki, Receiver operating characteristic (ROC) curve analysis for medical diagnostic test evaluation, Caspian Journal of Internal Medicine 4 (2) (2013) 627–635.